Oxidovanadium(IV/V) complexes of amino acid-based Schiff bases and aromatic heterocycles: DNA interactions and photocatalytic dye degradation

Susanta Das Baishnab[1,2], Anirban Chandra[1], Arjun Kumar De[2]
[1]*Department of Chemistry, Tripura University, Suryamaninagar 799022, Tripura, India*
[2]*Department of Science & Humanities, Tripura Institute of Technology, Narsingarh 799015, Tripura, India*
doi.org/10.64643/IJIRTV12I11-199410-459

***Abstract*—Two oxidovanadium complexes viz. [V^{V}OL(8-HQ)] (1) and [V^{IV}OL´(phen)] (2) (H_2L=2-(2-hydroxybenzylideneamino)-3-phenylpropanoic acid, H_2L´=2-(2-hydroxy-3-methoxybenzylideneamino)-3-phenylpropanoic acid, 8-HQ=8-hydroxy quinoline, phen=1,10-phenanthroline) were synthesized (Scheme 2) and characterized by elemental analyses and various spectroscopic techniques. Schiff base ligands H_2L and H_2L´ were prepared insitu by condensation of salicylaldehyde/ o-vanillin with L-phenylalanine in ethanol. Interaction of 1, 2 with DNA was ascertained by UV-visible and fluorescence spectroscopy. Photocatalytic dye degradation efficiency of complexes towards cationic and anionic organic dyes viz. methylene blue (MB) and brilliant blue (BB) was assessed under visible light by UV-visible spectroscopy. The degradation kinetics of the synthesized complexes were also evaluated using first order kinetic model. Both the complexes exhibit moderate dye degradation efficiency.**

***Index Terms*—Oxidovanadium, amino acid, Schiff base, binding constant, photocatalytic**.

I. INTRODUCTION

The study of transition metal complexes as therapeutics is a fascinating and promising field in biochemical research. In recent decades, there has been considerable progress in developing metal compounds as potential drugs for challenging diseases, such as parasitic infections, though progress in this field has remained relatively slow despite recent advancements [1-3]. A crucial step in drug design is to identify the drug's target. In cancer treatment, DNA is recognized as one of the primary targets. Therefore, the DNA binding and cleavage activity of redox-active metal compounds plays a vital role in the development of effective anticancer drugs. DNA cleavage can occur through hydrolytic or oxidative mechanisms, with an oxidative pathway being more prevalent for redox-active metal complexes. This discovery has significantly boosted the search for metallonucleases as potential anticancer therapies [4-11].

The interest in vanadium complexes in medicinal fields [12] is mainly due to their insulin-enhancing properties [13-16], potential antitumor [17-20] and antiparasitic effects [19-24], as well as their influence on various enzymes [25-28]. In recent decades, vanadium compounds have demonstrated beneficial in vitro effects in various animal cancer models and have provided protection at all stages of carcinogenesis [29]. For many decades, oxidovanadium(IV/V) complexes featuring salicylaldimine ligands derived from amino acids and aldehydes have attracted significant attention [30-37]. Oxidovanadium complexes with α-amino acid-based Schiff bases and planar N, O-donor heterocyclic bases as co-ligands have been well known for many decades [33,35,38] but have recently gained renewed attention [39-43]. This renewed interest is due to the heterocyclic base, which enables the complex to bind DNA via intercalation, surface binding, and groove binding [42].

Recently, researchers worldwide have focused on synthesizing metal−organic framework complexes to enhance the degradation or adsorption of dyes and remove them from chemically contaminated water [44-47]. Since synthetic dyes are widely used in

various industries, including paper, plastics, leather tanneries, food technology, and cosmetics [48,49], waste dyes are often released into rivers and ponds, leading to water contamination. These dye pollutants can cause a range of health issues in humans and animals, such as allergies, skin irritation, liver and kidney damage, and central nervous system disorders [50].

Therefore, considering the aforementioned aspects and building upon our ongoing interest in vanadium chemistry, the present work was undertaken. In this study, we report the synthesis and structural characterization of two α-amino acid-based Schiff base – oxidovanadium(IV/V) complexes, each containing an aromatic heterocycle as a co-ligand. Since DNA is the biological target of most anticancer drugs, the synthesized complexes were evaluated for their DNA binding ability using absorption and fluorescence emission spectroscopy. Additionally, the photocatalytic dye degradation properties of the complexes were examined against organic dyes such as methylene blue (MB) and brilliant blue (BB) to assess their effectiveness in degrading toxic dyes from aqueous solutions.

II. EXPERIMENTAL SECTION

Materials and Instrumentation

All the chemicals used, including calf thymus DNA (CT-DNA), dimethyl sulfoxide (DMSO), methylene blue (MB), brilliant blue (BB) and tris(hydroxymethylaminomethane) hydrochloride (Tris–HCl), are of analytical grade and were acquired from Sigma–Aldrich. Before being used, solvents were distilled. The magnetic susceptibility of the compounds was measured at room temperature using the Gouy method, employing a Sherwood Scientific Magnetic Susceptibility Balance, Model Auto and Revision 1.4.0, calibrated with $Hg[Co(SCN)_4]$ as the standard. The FT-IR spectra were recorded on a Bruker Alpha II FT-IR spectrophotometer. UV-visible spectra were recorded on a Shimadzu 1800 spectrophotometer. The fluorescence spectrophotometer model Fluorolog-3, Horiba Scientific, was used to record the fluorescence spectra. Electrospray ionization (ESI) mass spectra of the compounds were recorded on an XEVO G2-XS QTOF spectrometer in positive mode. C, H, and N contents in the obtained ligand and compound were ascertained by using a Perkin Elmer CHN analyzer (2400 series II). NMR spectra were recorded on Bruker Ascend™ at 400 MHz and 100 MHz, respectively. Vanadium was estimated by the gravimetric analysis method.

Synthesis

A solution (solution A) was prepared by refluxing (1 h) together a mixing of an aqueous solution (5 mL) of L-phenylalanine (1 mmol, 0.165 g) and an ethanolic solution (10 mL) of salicylaldehyde (1 mmol, 0.122 g) in the case of **1**/o-vanillin (1 mmol, 0.152 g) in the case of **2**. Another solution (solution B) was prepared by dissolving $VOSO_4$, H_2O (1 mmol, 0.181g) in water. The solutions A & B were mixed together, followed by the addition of a methanolic solution (5 mL) of 8-hydroxy quinoline (1 mmol, 0.145 g) for **1** and 1,10-phenanthroline (1 mmol, 0.180 g) for **2** with stirring. The resultant reaction mixture was further stirred at room temperature for ca. 3 hrs when a dark blue (for **1**)/dark red (for **2**) coloured clear solution was obtained. The solution was filtered and left undisturbed at room temperature for slow evaporation. After a few days, a dark blue (for **1**) and dark red (for **2**) microcrystalline solid separated out. Products were filtered, washed with ethanol, and dried over anhydrous $CaCl_2$.

$[V^{V}OL(8\text{-}HQ)]$ (1): Yield~ 68%. Anal. Calcd for $C_{25}H_{19}N_2O_5V$ Found (Calcd) (%): C 66.63 (66.87); H 3.96 (3.94); N 5.84 (5.87); V 10.64 (10.60).

$[V^{IV}OL'(phen)]$ (2): Yield~ 70%. Anal. Calcd for Anal. Calcd for $C_{29}H_{23}N_3O_5V$ Found (Calcd) (%): C 63.85 (63.68); H 4.22 (4.24); N 7.71 (7.65); V 9.35 (9.31).

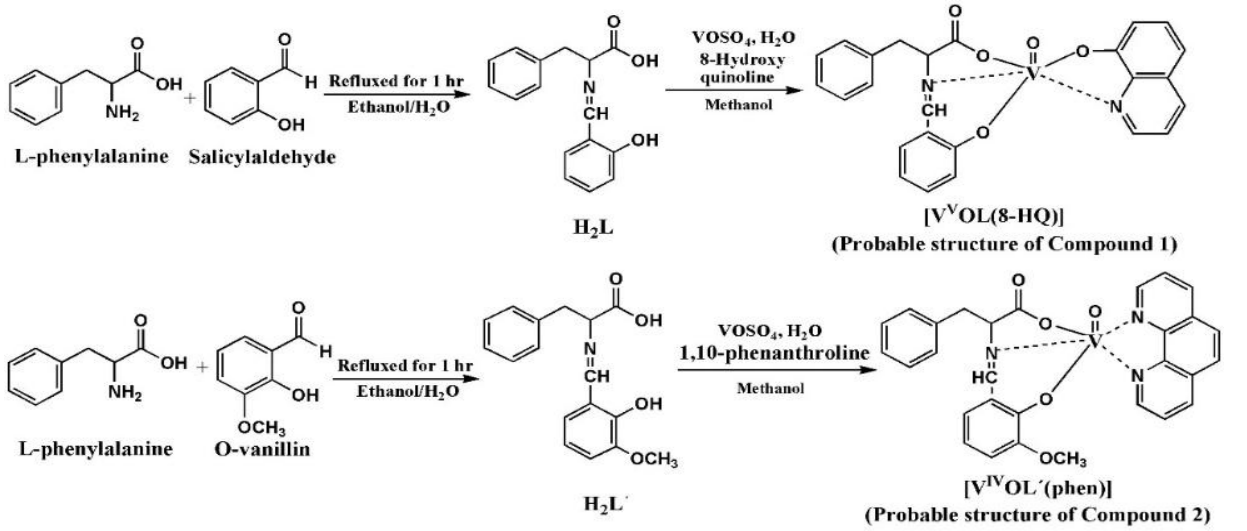

Scheme 1. The schematic diagram of pathways by which the oxidovanadium complexes (**1**, **2**) were synthesized.

III. RESULTS AND DISCUSSION

SYNTHESIS

Two oxidovanadium complexes were prepared in situ using a common synthetic procedure [51] for each set by reaction of a stoichiometric amount of the monohydrated vanadyl sulfate ($VOSO_4.H_2O$) with the corresponding ligand (and co-ligand); their structural formulae are depicted in Scheme 1. The resulting complexes, **1** and **2**, precipitated as blue and red microcrystalline solids, respectively, in good yields, were soluble in chloroform, and were characterized by elemental analysis, UV–visible, FTIR spectroscopies, ESR, and mass spectrometry.

SPECTROSCOPIC CHARACTERIZATION

Infrared Spectroscopy

FT-IR spectra of the complexes were recorded in KBr pressed pellets, as shown in Fig. 1. The FT-IR of complexes **1** and **2** displayed strong absorptions at ca 1700 and 1250 cm^{-1} assignable to ν(C=O) and ν(C–O)$_{phenolic}$ stretching vibrations, respectively. The characteristic terminal ν(V=O) band appears as a strong band at 975 and 950 cm^{-1}, respectively. The $\nu_{asym}(CO_2)$ and $\nu_{sym}(CO_2)$ stretching of COO^- moiety of the amino acid residue appeared at 1630-1640 and 1370-1384 cm^{-1}, respectively which were shifted in comparison to the non-coordinated amino acid, suggests coordination of COO^- to the metal center [37,38,52]. The strong band at 1600 cm^{-1} is assignable to ν(C=N), indicating the condensation of the carbonyl group of aldehyde with -NH_2 of amino acid and the coordination of imine N (C=NH-) to the metal center. Additional absorptions at 1540-1550, 745-760, and 685-690 cm^{-1} are assignable to ν(C=C/aromatic), ν_{asym}(V–O), and ν_{sym}(V–O) stretching vibrations, respectively.

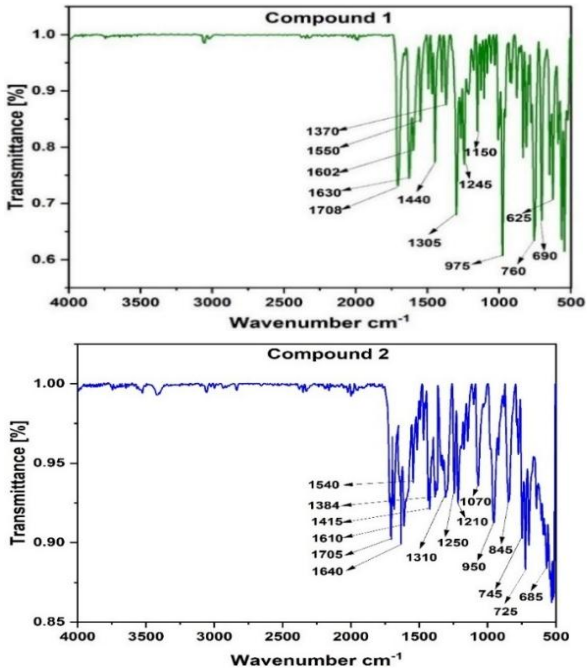

Fig. 1. FT-IR spectra of compounds **1** and **2**.

Electronic Spectra

The electronic spectra of the complexes were recorded in a DMSO solution (10^{-5} M) at room temperature, as shown in Fig. 2. The absorption spectra of the

complexes show a strong band at 285-340 nm for **1** & **2** and a broad band for complex **2** at 420 nm, assigned to intra-ligand π–π* and d-d transitions, respectively.

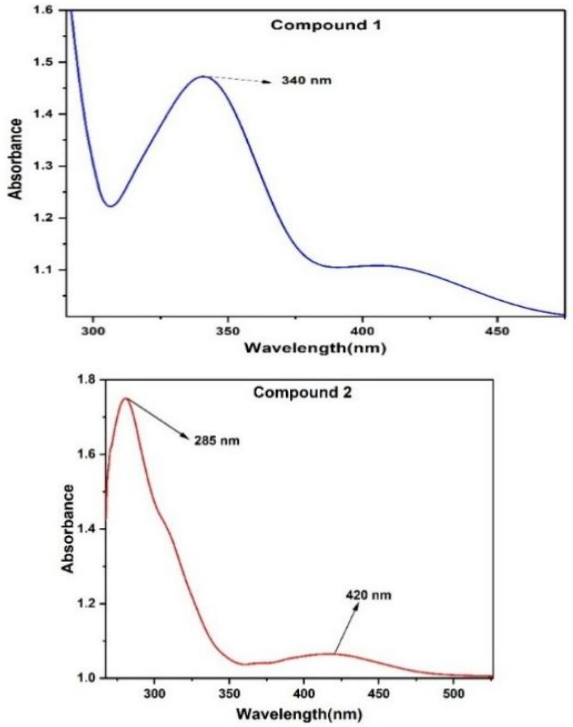

Fig. 2. UV-visible spectra of compounds **1** and **2**.

Mass Spectrometry

Mass spectrometry is widely recognized as a powerful technique for the structural elucidation of molecules in molecular chemistry. Its application has proven to be particularly effective in coordination chemistry, especially in determining the primary molecular ion peaks of Schiff base metal complexes. The analysis was conducted using electrospray ionization mass spectrometry (ESI-MS). The molecular ion peaks observed in the mass spectra of compounds **1** and **2** show strong agreement with the calculated values, as illustrated in Fig. 3. The mass spectrum of **1** shows a prominent peak at m/z ~479, corresponding to $[C_{25}H_{19}N_2O_5V]+H^+$ ($M+H^+$). For complex **2** the peak at m/z at ~545 is assigned as $[C_{29}H_{23}N_3O_5V]+H^+$ and agrees with the molecular composition of the complexes. Fragments at m/z ~213 and ~335 are due to $[C_9H_6NO_2V]+H^+$ and $[C_{16}H_{13}NO_4V]+H^+$ (compound **1**), whereas peaks at m/z ~247 and ~366 were assignable to $[C_{12}H_8N_2OV]+H^+$ and $[C_{17}H_{15}NO_5V]+H^+$ for compound **2**. Thus, mass spectrometric data lend support to the molecular composition of the complexes.

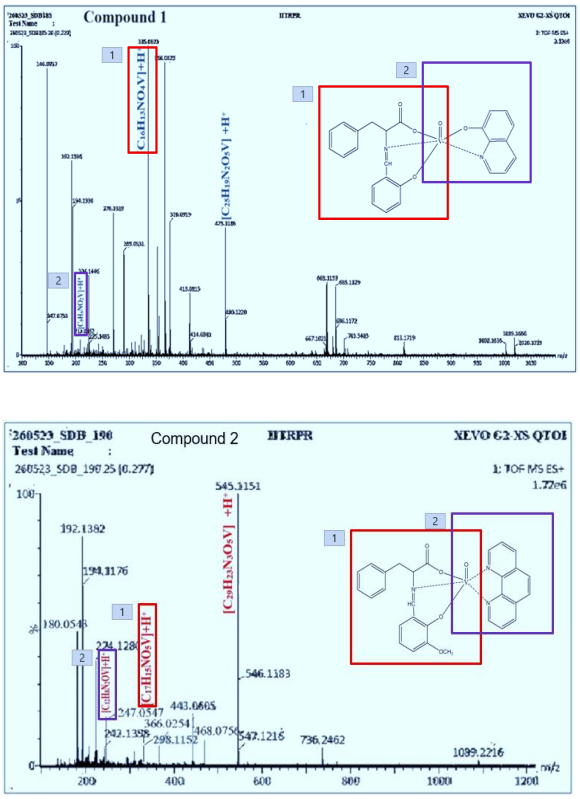

Fig. 3. Mass spectra of compounds **1** and **2**.

ESR Spectra

Electron Spin Resonance spectral studies of complex 1, show the compound is ESR silent. The solid-state Electron Spin Resonance (ESR) spectra of the complex 2, as shown in Fig. 4, recorded at room temperature, exhibit a g-value of 1.977. This g-value is consistent with the presence of vanadium(IV) in Complex 2. Vanadium(IV), in a typical coordination environment, often exhibits an ESR spectrum with g-values in the range of approximately 1.95–2.00, which matches well with the observed value in this case. These suggest that the vanadium centers in the complexes 1 & 2 are in the +5 and +4 oxidation states, respectively.

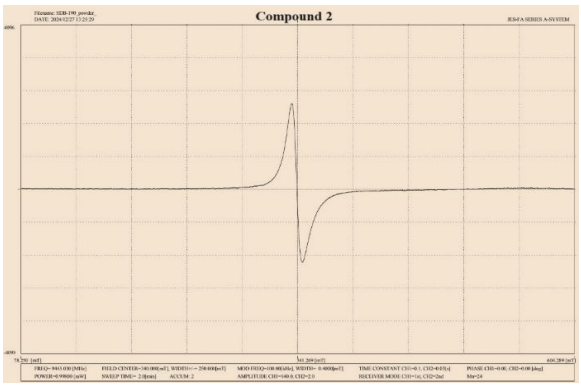

Fig. 4. ESR spectrum of compound 2.

Room temperature Magnetic moment

The room temperature magnetic moment values of complexes **1** and **2** were found to be zero and 1.85 BM, respectively. The observed values indicate the presence of vanadium(V) and vanadium(IV) centres in complexes **1** and **2**, respectively.

SEM- EDAX analyses

Morphological features and elemental compositions of the complexes were ascertained using SEM-EDAX. SEM images (Figs. 5 and 6) indicate the compound consists of irregular block-type aggregates. The elemental analysis data obtained from EDAX are consistent with the molecular compositions of the complexes.

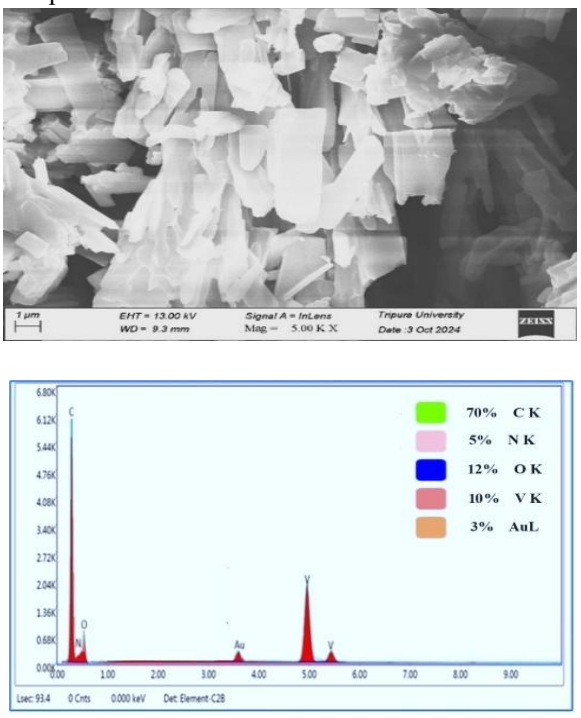

Fig. 5. SEM image of compound **1** and percentage composition obtained from EDAX.

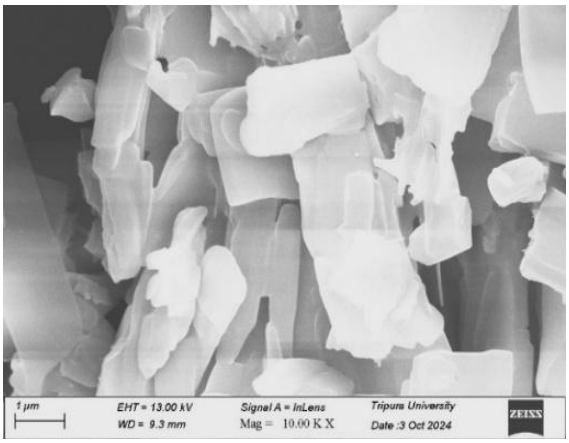

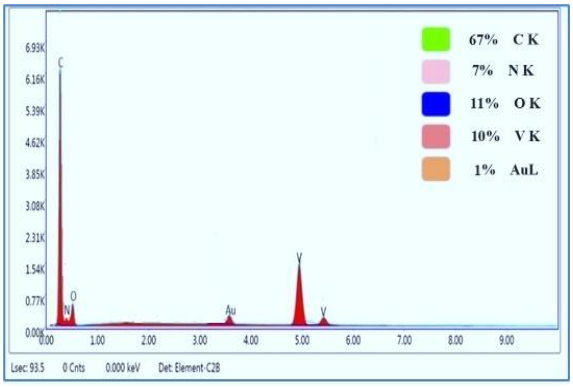

Fig. 6. SEM image of compound **2** and percentage composition obtained from EDAX.

DNA BINDING ABILITY AND INTERACTION MODE

Spectrophotometric studies on DNA binding

Electronic absorption titration is a widely used technique to study the interaction between calf thymus DNA (CT-DNA) and metal compounds [53]. The absorption spectra usually show a red or blue shift and a hypochromic or hyperchromic effect when small molecules intercalate with CT-DNA [54]. The DNA binding study of complexes **1** and **2** reveals their potential to interact with CT-DNA. The addition of oxovanadium compounds to a CT-DNA solution likely forms a ground state complex, referred to as the DNA-drug complex, where "drug" represents one of the oxovanadium complexes **1** or **2**. The absorption characteristics of the interaction between CT-DNA and complexes **1** and **2** at various concentrations, along with the blank tests in the absence of **1** and **2**, are shown in Fig. 7. A hyperchromic effect is observed upon adding oxovanadium complexes to CT-DNA. This effect can be attributed to external contact

(surface binding) with the duplex DNA. The changes in the absorption pattern of CT-DNA upon the addition of the complexes, without any shift in the peak position (258 nm), suggest that the interaction likely occurs through a non-intercalating binding mode on the periphery of the double helix [55,56]. The degree of hyperchromism supports a non-intercalative binding mode, indicating that the binding of the synthesized compounds to CT-DNA is likely facilitated by electrostatic, Van der Waals, and hydrogen bonding interactions [57] .

The apparent association constant (K_{app}) for the formation of DNA-drug between CT-DNA and the oxovanadium complexes is represented by equation 2.

CT-DNA + drug DNA-drug (1)

K_{app} = [DNA-drug] / [CT-DNA] × [drug] (2)

The K_{app} is obtained based on Benesi and Hildebrand's method [58].

$A_{obs} = (1-\alpha)C_0\varepsilon_{DNA}l + \alpha C_0\varepsilon_c l$ (3)

Herein, A_{obs} is the observed absorbance of the solution, containing various concentrations of oxovanadium complexes (drug) at 258 nm, α is the degree of association between CT-DNA and drug, ε_{DNA} and ε_c are the molar extinction coefficients at the defined wavelength (λ = 258 nm) for CT-DNA and the formed compound, respectively, 'l' is the optical path length, and C_0 is the primary concentration of CT-DNA. Equation 3 can be expressed as follows:

$A_{obs} = (1-\alpha)\ A_0 + \alpha A_c$ (4)

where, A_0 and A_c are the absorbances of CT-DNA and the compound at 258 nm, respectively, having a concentration of C_0.

Further, α can be equated to (K_{app}[drug])/ (1 + K_{app}[drug]). Thus, Equation 2 is changed to [59]:

$1/A_{obs}-A_0 = 1/A_c-A_0 + 1/K_{app}(A_c-A_0) \times 1/[drug]$ (5)

On enhancement of the absorbance at 258 nm due to absorption of the DNA-drug complex, a linear relationship between the reciprocal concentration of drug $1/(A_{obs} - A_0)$, slope $1/K_{app}(A_c - A_0)$, and an intercept $1/(A_c - A_0)$ is expected (Fig. 7, insets). The determined values of the apparent association constants (K_{app}) are summarized in Table 1. The K_{app} values for the oxovanadium complexes are approximately in the range of 10^4. This suggests a moderate binding of **1** and **2** to CT-DNA.

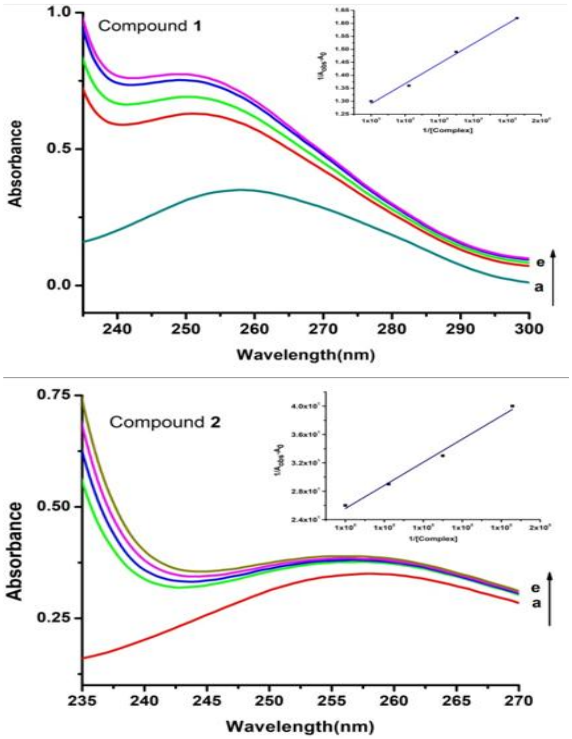

Fig. 7. UV-visible spectra of CT-DNA (1×10^{-5} M) in the presence of incremental amounts of complex **1**, **2** (curves a–e). Insets represent plot of $1/(A_{obs}-A_0)$ vs 1/[Complex].

Table 1. Apparent binding constants (K_{aap}) for interaction of **1**, **2** with CT-DNA

Compound	Binding constant (M-1)	R2
1	6.6845×10^4	0.97948
2	2.2646×10^4	0.98921

Fluorescence studies

Fluorescence spectra were obtained to investigate the interaction between oxovanadium complexes **1** and **2** and CT-DNA (calf thymus DNA). Fluorescent compounds like methylene blue (MB) or ethidium bromide (EB) are commonly used to study the interaction between dyes and DNA. In this case, fluorescence measurements were conducted using methylene blue (MB) as a probe, which binds with CT-DNA to form a (DNA–MB) adduct. During the emission measurement, the concentration of the (DNA–MB) adduct solution was kept constant, while the concentration of the oxovanadium complexes was varied. The fluorescence emission spectra of the DNA-MB solution in the presence of increasing concentrations of **1** and **2** are presented in Fig. 8.

Upon binding to CT-DNA, the fluorescence of methylene blue is typically quenched [60]. If the interaction between the oxovanadium complexes and DNA-MB results in the separation of methylene blue from DNA, a notable increase in MB emission would be expected. However, in this case, no significant increase in the fluorescence intensity of methylene blue is observed upon adding increasing concentrations of compounds 1 and 2, likely due to the limited release of MB from the DNA-MB complex. Therefore, the fluorescence measurements do not offer further insight into the nature of the interaction between CT-DNA and compounds 1 and 2.

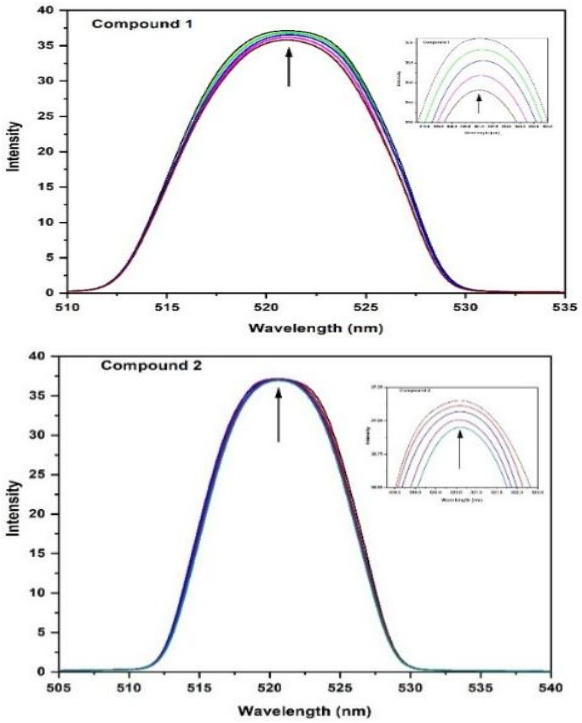

Fig. 8. Emission spectra of the DNA-MB complex with increasing amounts of compounds **1** and **2**. [CT-DNA] = [MB] = 5 ×10^{-5} M and λ_{ex}= 512 nm.

PHOTOCATALYTIC DYE DEGRADATION ACTIVITY

The photocatalytic degradation activity of cationic and anionic dyes, such as methylene blue (MB) and brilliant blue (BB), was evaluated using the synthesized oxidovanadium complexes (**1** and **2**) under visible light, with the progress monitored by UV-visible absorption spectroscopy [61,62]. The dye molecules have characteristic absorption peaks, and the absorbance of the dyes at their initial concentration was measured. The interaction of the aqueous solution of the dyes in the presence of the catalytic amount of the complexes shows a decrease in absorbance under visible light as the duration of the exposure to light increases (Figs. 9 and 10).

The gradual decrease in absorbance of the dyes with decolorization during the process provides strong evidence for efficient degradation of dyes by the complexes.

The photocatalytic degradation efficiency (D_e) of complexes was determined using the equation [63]:

$D_e = [\{(C_0-C_t)/C_0\} \times 100] \% = [\{(A_0-A_t)/A_0\} \times 100] \%$

The initial concentration of the dye solution is represented by C_0 and the concentration after adsorption at time t by C_t, while the absorbance of the dye before and after adsorption is represented by A_0 and A_t, respectively. The photodegradation efficiency of complexes **1** and **2** toward MB (in 50 min) was determined to be 54.79% and 56.57%, respectively. For BB, the degradation efficiency of complexes **1** and 2 was found to be 45.74% and 45.48%, respectively.

The degradation kinetics of the synthesized complexes were evaluated using first order kinetic model.

$\ln (A_t/A_0) = -kt$

where, A_0 is the initial absorbance of dye solution and A_t is the absorbance of the dye solution at time t (min). The plot of $\ln(A_t/A_0)$ versus time for a given dye concentration (Figs. 11 and 12), along with their linear fit provide the apparent rate constants for dye degradation [64] (Table 2). The degradation rate constants (k) for degradation of MB and BB by compound **1** are found to be 1.804 x 10^{-2} min^{-1} and 1.148 x 10^{-2} min^{-1}, respectively. Similarly, degradation rate constants (k) for degradation of MB and BB by compound **2** are found to be 1.674 x 10^{-2} min^{-1} and 1.175 x 10^{-2} min^{-1}, respectively. The degradation rate of MB using both compounds was found to be higher than that of BB.

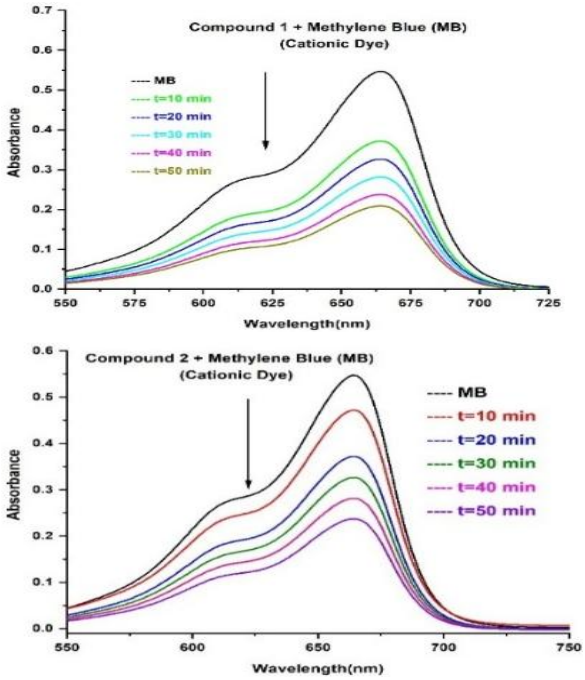

Fig. 9. UV-visible spectra of the aqueous MB dye solution during the photodegradation study with complexes.

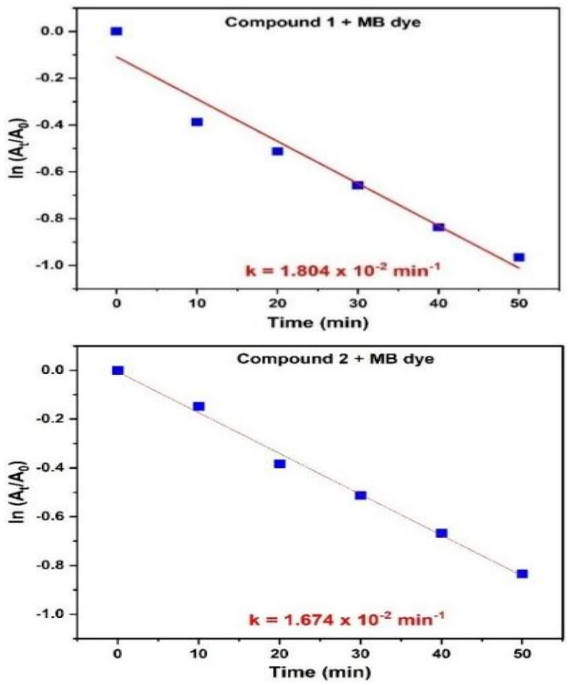

Fig. 11. Plots of ln (A_t /A_0) vs. time for the degradation of MB dye (λ_{max} = 664 nm) by complexes (1, 2).

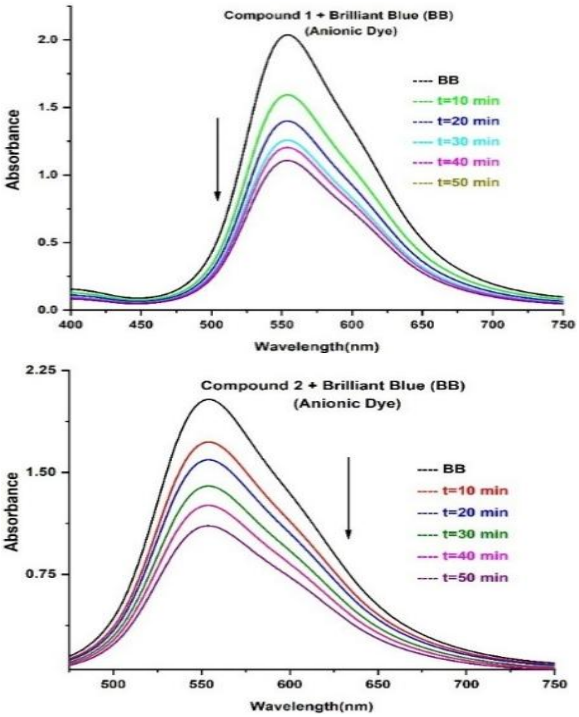

Fig. 10. UV-visible spectra of the aqueous BB dye solution during the photodegradation study with complexes.

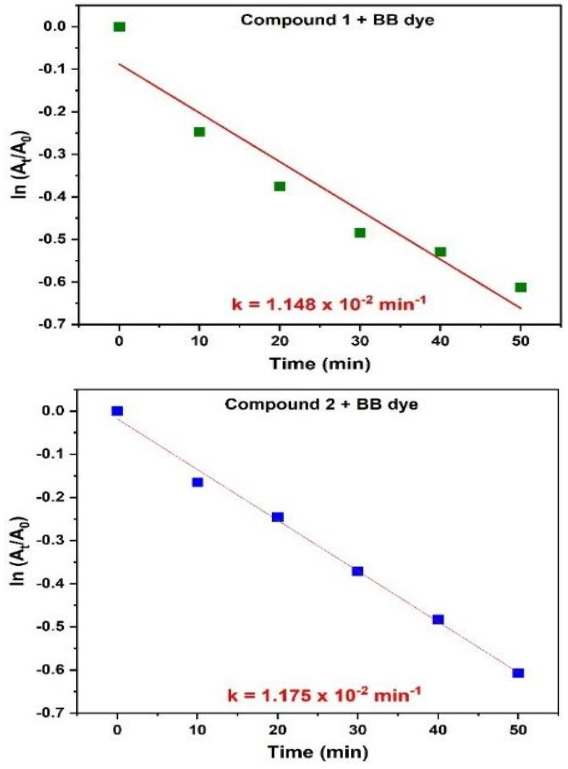

Fig. 12. Plots of ln (A_t /A_0) vs. time for the degradation of BB dye (λ_{max} = 553 nm) by complexes (1, 2).

Table 2. Photocatalytic dye degradation rate constants and its efficiency under visible light

Photocatalyst	Dye	Concentration of dye (mg/L)	Amount of Photocatalyst (mg)	Kinetic rate constant (x 10^{-2} min^{-1})	Degradation efficiency (%)
Compound **1**	MB	0.02	10	1.804	54.79
	BB			1.148	45.74
Compound **2**	MB	0.02	10	1.674	56.57
	BB			1.175	45.48

IV. CONCLUSION

Two oxidovanadium complexes viz., [V^{V}OL(8-HQ)] (**1**) and [V^{IV}OL′(phen)] (**2**) (H_2L = 2-(2-hydroxybenzylideneamino)-3-phenylpropanoic acid, H_2L'=2-(2-hydroxy-3-methoxybenzylideneamino)-3-phenylpropanoic acid, 8-HQ=8-hydroxy quinoline, and phen=1,10-phenanthroline) were synthesized and comprehensively characterized by elemental analyses and various spectroscopic techniques. Schiff base ligands H_2L and H_2L' were prepared in situ by condensation of salicylaldehyde/ o-vanillin with L-phenylalanine in ethanol. Interaction of **1** and **2** with DNA was ascertained by UV-visible and fluorescence spectroscopy. Photocatalytic dye degradation efficiency of complexes towards cationic and anionic organic dyes, viz., methylene blue (MB) and brilliant blue (BB), was assessed under visible light by UV-visible spectroscopy. The degradation kinetics of the synthesized complexes were also evaluated using the first-order kinetic model. Both the complexes exhibit moderate dye degradation efficiency.

V. ACKNOWLEDGEMENTS

The authors are thankful to the authority of Tripura University, Suryamaninagar and Central Instrumentation Center, Tripura University for providing infrastructure facility.

VI. CONFLICT OF INTEREST

The authors declare no conflict of interest.

REFERENCES

[1] D. Crespy, K. Landfester, U. S. Schubert, A. Schiller, Potential photoactivated metallopharmaceuticals: from active molecules to supported drugs. *Chem. Commun*., 46 (2010) pp. 6651–6662.

[2] D. Gambino, Potentiality of vanadium compounds as anti-parasitic agents. *Coord. Chem. Rev*., 255 (2011) pp. 2193–2203.

[3] B. Gyurcsik, A. Czene, Towards Artificial Metallonucleases for Gene Therapy: Recent Advances and New Perspectives. *Future Med. Chem.*, 3 (2011) pp. 1935–1966.

[4] J. C. Dabrowiak, Metals in Medicine. *Wiley*, 2009.

[5] B. K. Keppler, Coordination chemistry of metallodrugs: insights into biological speciation from NMR spectroscopy. *VCH, Weinheim and New York,*1993.

[6] F. Mancin, P.Scrimin, P.Tecilla, Progress in artificial metallonucleases. *Chem. Commun*., 48 (2012) pp. 5545–5559.

[7] N. Butenko, A. I. Tomaz, O. Nouri, E. Escribano, V. Moreno, S. Gama, V.Ribeiro, J. P. Telo, J. Costa Pessoa, I. Cavaco, DNA cleavage activity of $V^{IV}O(acac)_2$ and derivatives. *J. Inorg. Biochem*., 103 (2009) pp. 622–632.

[8] S. Gama, F. Mendes, F. Marques, I. C. Santos, M. F. Carvalho, I. Correia, J. Costa Pessoa, I. Santos, A. Paulo, Copper (II) complexes with tridentate pyrazole-based ligands: synthesis, characterization, DNA cleavage activity and cytotoxicity, *J. Inorg. Biochem*., 105 (2011) pp. 637–644.

[9] K. Paliwal, A. Swain, D. P. Mishra, P. K. S. Antharjanam, M. Kumar, A novel copper(ii) complex with a salicylidene carbohydrazide ligand that promotes oxidative stress and apoptosis in triple negative breast cancer cells, *Dalton Trans.*, 53 (2024) pp. 17702-17720.

[10] J. Z. Lu, H. W. Guo, X. D. Zeng, Y. L. Zhang, P. Zhao, J. Jiang, L. Q. Zang, Synthesis and characterization of unsymmetrical oxidovanadium complexes: DNA-binding,

cleavage studies and antitumor activities. *J. Inorg. Biochem*., 112 (2012) pp. 39–48.

[11] A. Terenzi, M. Fanelli, G. Ambrosi, S. Amatori, V. Fusi, L. Giorgi, V. T. Liveri, G. Barone, DNA binding and antiproliferative activity toward human carcinoma cells of copper(ii) and zinc(ii) complexes of a 2,5-diphenyl [1,3,4] oxadiazole derivative. *Dalton Trans*., 41 (2012) pp. 4389–4395.

[12] J. Costa Pessoa, S. Etcheverry, D. Gambino, Vanadium compounds in medicine. *Coord. Chem. Rev*., (2015)

[13] Y. Shechter, A. Shisheva, Vanadium salts and the future treatment of diabetes, *Endeavour*, 17 (1993) pp. 27–31.

[14] K. H. Thompson, J. H. Mc Neill, C. Orvig, Vanadium Compounds as Insulin Mimics, *Chem. Rev*., 99 (1999) pp. 2561–2572.

[15] L. M. P. F. Amaral, T. Moniz, A. M. N. Silva, M. Rangel, Vanadium Compounds with Antidiabetic Potential, *Int. J. Mol. Sci.*, 24 (2023) 15675.

[16] A. M. A. Adam, A. M. Naglah, M. A. Al-Omar, M. S Refat, Synthesis of a new insulin-mimetic anti-diabetic drug containing vitamin A and vanadium (IV) salt: Chemico-biological characterizations, *Int. J. Immun. Pharm*., 30 (2017) pp. 272-281.

[17] A. M. Evangelou, Vanadium in cancer treatment, *Crit. Rev. Oncol. Hematol*., 42 (2002) pp. 249–265.

[18] I. Kostova, Ruthenium complexes as anticancer agents, *Anticancer Agent Med. Chem*., 9 (2009) pp. 827–842.

[19] G. Scalese, I. Correia, J. Benítez, S. Rostán, F. M arques, F. Mendes, A. P. Matos, J. C. Pessoa, D. Gambino, Evaluation of cellular uptake, cytotoxicity and cellular ultrastructural effects of heteroleptic oxidovanadium(IV) complexes of salicylaldimines and polypyridyl ligands, *J. Inorg. Biochem*., 166 (2017) pp. 162-172.

[20] J. Benitez, L. Guggeri, I. Tomaz, J. Costa Pessoa, V. Moreno, J. Lorenzo, F. X. Aviles, B. Garat, D. Gambino, A novel vanadyl complex with a polypyridyl DNA intercalator as ligand: A potential anti-protozoa and anti-tumor agent, *J. Inorg. Biochem*., 103 (2009) pp. 1386–1394.

[21] J. Benitez, A. C. De Queiroz, I. Correia, M. A. Alves, M. S. Alexandre-Moreira, E. J. Barreiro, L. M. Lima, J. Varela, M. Gonzalez, H. Cerecetto, V. Moreno, J. Costa Pessoa, D. Gambino, New oxidovanadium(IV) N-acylhydrazone complexes: Promising antileishmanial and antitrypanosomal agents, *Eur. J. Med. Chem*., 62 (2013) pp. 20–27.

[22] M. Fernandez, L. Becco, I. Correia, J. Benitez, O. E. Piro, G. A. Echeverria, A. Medeiros, M. Comini, M. L. Lavaggi, M. Gonzalez, H. Cerecetto, V. Moreno, J. Costa Pessoa, B. Garat, D. Gambino, Oxidovanadium(IV) and dioxidovanadium(V) complexes of tridentate salicylaldehyde semicarbazones: Searching for prospective antitrypanosomal agents, *J. Inorg. Biochem*., 127 (2013) pp. 150–160.

[23] J. Benitez, I. Correia, L. Becco, M. Fernandez, B. Garat, H. Gallardo, G. Conte, M. L. Kuznetsov, A. Neves, V. Moreno, J. Costa Pessoa, D. Gambino, Vanadium-Based Prospective Agents against Trypanosoma cruzi: Oxidovanadium(IV) Compounds with Phenanthroline Derivatives as Ligands, *Z. Anorg. Allg. Chem*., 639 (2013) pp. 1417-1425.

[24] M. Fernandez, J. Varela, I. Correia, E. Birriel, J. Castiglioni, V. Moreno, J. Costa Pessoa, H. Cerecetto, M. Gonzalez, D. Gambino, A new series of heteroleptic oxidovanadium(iv) compounds with phenanthroline-derived co-ligands: selective Trypanosoma cruzi growth inhibitors. *Dalton Trans*., 42 (2013) pp. 11900–11911.

[25] D. C. Crans, J. J. Smee, E. Gaidamauskas, L. Q. Yang, The Chemistry and Biochemistry of Vanadium and the Biological Activities Exerted by Vanadium Compounds, *Chem. Rev*., 104 (2004) pp. 849–902.

[26] D. C. Crans, M. L. Tarlton, C. C. Mc Lauchlan, Trigonal Bipyramidal or Square Pyramidal Coordination Geometry? Investigating the Most Potent Geometry for Vanadium Phosphatase Inhibitors, *Eur. J. Inorg. Chem*., 27 (2014) pp. 4450–4468.

[27] J. Costa Pessoa, E. Garriba, M. F. A. Santos, T. Santos-Silva, Vanadium and proteins: Uptake, transport, structure, activity and function, *Coord. Chem. Rev*., 301-302 (2015) pp. 49-86.

[28] C. C. Mc Lauchlan, B. J. Peters, G. R. Willsky, D. Crans, Vanadium–phosphatase complexes: Phosphatase inhibitors favor the trigonal

bipyramidal transition state geometries, *Coord. Chem. Rev*., 301-302 (2015) pp. 163-199.

[29] A. Bishayee, A. Waghray, M. A. Patel, M. Chatterjee, Vanadium in the detection, prevention and treatment of cancer: The in vivo evidence, *Cancer Lett*., 294 (2010) pp. 1–12.

[30] L. J. Theriot, G. O. Carlisle, H. J. Hu, Oxovanadium (IV) complexes with N-salicylideneamino acids, *J. Inorg. Nucl. Chem*., 31 (1969) pp. 2841-2844.

[31] S. Mondal, S. Dutta, A. Chakravorty, Synthesis and structure of carboxyl-bonded oxovanadium(V) complexes incorporating α-amino acid salicylaldiminates and quinolin-8-olate, *J. Chem. Soc. Dalton Trans*., 7 (1995) pp. 1115–1120.

[32] S. Dutta, S. Mondal, A. Chakravorty, Chemistry of VO3+ and VO2+ complexes incorporating N-salicylidene-α-aminoacidates, *Polyhedron*, 14 (1995) pp. 1163–1168.

[33] I. Cavaco, J. Costa Pessoa, D. Costa, M. T. Duarte, R. D. Gillard, P. Matias, N-salicylideneamino acidate complexes of oxovanadium(IV). Part 1. Crystal and molecular structures and spectroscopic properties, *J. Chem. Soc. Dalton Trans.*, 2 (1994) pp. 149–157.

[34] M. A. Hasan, H. Rahman, M. M. Haque, M. N. Islam, Synthesis, Characterization and In-vitro Antibacterial Activity Studies of Oxovanadium (IV) Complexes of α-Amino Acid Schiff Bases and 1,10-Phenanthroline Ligands, *Asian J. Chem. Sci*., 14 (2024) pp. 68-82.

[35] I. Cavaco, J. Costa Pessoa, M. T. Duarte, R. T. Henriques, P. M. Matias, R. D. Gillard, Crystal and molecular structure of [V2O3(sal-L-val)2(H2O)](sal-L-val =N-salicylidene-L-valinate) and spectroscopic properties of related complexes, *J. Chem. Soc. Dalton Trans.*, 9 (1996) pp. 1989–1996.

[36] J. Costa Pessoa, I. Cavaco, I. Correia, M. T. Duarte, R. D. Gillard, R. T. Henriques, F. J. Higes, C.Madeira, I. Tomaz, Preparation and characterisation of new oxovanadium (IV) Schiff base complexes derived from amino acids and aromatic o-hydroxyaldehydes, *Inorg. Chim. Acta*, 293 (1999) pp. 1–11.

[37] J. Costa Pessoa, M. J. Calhorda, I. Cavaco, I. Correia, M. T. Duarte, V. Felix, R. T. Henriques, M. F. M. Piedade, I. T omaz, Molecular modelling studies of N-salicylideneamino acidato complexes of oxovanadium(iv). Molecular and crystal structure of a new dinuclear LOVIV–O–VVOL mixed valence complex, *J. Chem. Soc. Dalton Trans.*, 23 (2002) pp. 4407–4415.

[38] Costa Pessoa, M. J. Calhorda, I. Cavaco, P. J. Costa, I. Correia, D. Costa, L. F. Vilas-Boas, V. Felix, R. D. Gillard, R. T. Henriques, R. Wiggins, N-Salicylideneamino acidato complexes of oxovanadium(iv). The cysteine and penicillamine complexes, *Dalton Trans*., 18 (2004) pp. 2855–2866.

[39] A. R. Chakravarty, Photocleavage of DNA by copper (II) complexes, *J. Chem. Sci*., 118 (2006) pp. 443–453.

[40] P. A. N. Reddy, M. Nethaji, A. R. Chakravarty, Hydrolytic Cleavage of DNA by Ternary Amino Acid Schiff Base Copper (II) Complexes Having Planar Heterocyclic Ligands, *Eur. J. Inorg. Chem*., (2004) pp. 1440–1446.

[41] P. A. N. Reddy, M. Nethaji, A. R. Chakravarty, Synthesis, crystal structures and properties of ternary copper (II) complexes having 2,2′-bipyridine and α-amino acid salicylaldiminates as models for the type-2 sites in copper oxidases, *Inorg. Chim. Acta*, 337 (2002) pp. 450–458.

[42] P. K. Sasmal, A. K. Patra, M. Nethaji, A. R. Chakravarty, DNA Cleavage by New Oxovanadium (IV) Complexes of N-Salicylidene α-Amino Acids and Phenanthroline Bases in the Photodynamic Therapy Window, *Inorg. Chem*., 46 (2007) pp. 11112–11121.

[43] U. Saha, T. K. Si, P. K. Nandi, K. K. Mukherjea, an amino acid coordinated vanadium (IV) complex: Synthesis, structure, DFT calculations and VHPO mimicking catalytic bromoperoxidation of organic substrates, *Inorg. Chem. Commun*., 38 (2013) pp. 43–46.

[44] M. Z. Wu, J. Y. Shi, P. Y. Chen, L. Tian, Two 3D Cobalt (II) Metal–Organic Frameworks with Micropores for Selective Dye Adsorption, *J. Chen, Inorg. Chem*., 58 (2019) pp. 3130−3136.

[45] S. Tanaka, H. Sato, Y. Ishida, Y. Deng, T. Haraguchi, T. Akitsu, M. Sugiyama, M. Hara, D. Moon, Photo-Control of Adsorption of Dye Metal Complexes Incorporating Chiral Schiff Base Ligands Containing Azo-Groups on TiO2, *J. Korean Chem. Soc*., 62 (2018) pp. 328−332.

[46] F. Deng, X. Qin, K. Chai, Z. Wei, K. Wang, B. Liao, J. Wu, Z. Pang, F. Shen, Adsorption and Removal of Industrial Dyes by Water-Stabilized Aluminum-Based Metal–Organic Frameworks, *ACS Applied Nano Mat*., 6 (2023) pp. 8675–8684.

[47] A. Beheshti, E. S. M. Fard, M. Kubicki, P. Mayer, C. T. Abrahams, S. E. Razatofighi, Design, synthesis and characterization of copper-based coordination compounds with bidentate (N,N and N,O) ligands: reversible uptake of iodine, dye adsorption and assessment of their antibacterial properties, *Cryst. Eng. Comm*., 21 (2019) pp. 251−262.

[48] C. -Y. Yue, X.-W. Lei, Y.-F. Han, X.-X. Lu, Y.-W. Tian, J. Xu, X.-F. Liu, X. Xu, Transition-Metal-Complex Cationic Dyes Photosensitive to Two Types of 2D Layered Silver Bromides with Visible-Light-Driven Photocatalytic Properties, *Inorg. Chem*., 55 (2016) pp. 12193− 12203.

[49] S. Pathak, M. K. Ghosh, T. K. Ghorai, Luminescence, Dye Degradation and DNA Binding Properties of a Dinuclear Nona-Coordinated Y(III) Complex, *Chemistry Select*, 3 (2018) pp. 13501−13506.

[50] C. Umamaheswari, A. Lakshmanan, N. S. Nagarajan, Green synthesis, characterization and catalytic degradation studies of gold nanoparticles against congo red and methyl orange, *J. Photochem. Photobiol*. B, 178 (2018) pp. 33−39.

[51] J. Costa Pessoa, I. Cavaco, I. Correia, M.T. Duarte, R.D. Gillard, R.T. Henriques, F.J. Higes, C. Madeira, I. Tomaz, Preparation and characterisation of new oxovanadium (IV) Schiff base complexes derived from amino acids and aromatic o-hydroxyaldehydes, *Inorg. Chim. Acta* 293 (1999) pp. 1–11.

[52] K. Nakamoto, Infrared and Raman Spectra of Inorganic and Coordination Compounds, *Wiley*, (2006).

[53] J. K. Barton, A. T. Danishefsky, G. M. Goldburg, Tris(phenanthroline)ruthenium (II): stereoselectivity in binding to DNA, *J. Am. Chem. Soc*., 106 (1984) pp. 2172-2176.

[54] R. Fekri, M. Salehi, A. Asadi, M. Kubieki, Protein-polyelectrolyte complexes: Molecular dynamics simulations and experimental study, *Polyhedron*, 128 (2017) pp. 175-187.

[55] M. D'Abramo, Ch. L. Castellazzi, M. Orozco, A. Amadei, On the Nature of DNA Hyperchromic Effect, *Phys. Chem*., 117 (2013) pp. 8697–8704.

[56] M. F. Dehkordi, G. Dehghan, M. Mahdavi, M. A. Hosseinpour Feizi, Multispectral studies of DNA binding, antioxidant and cytotoxic activities of a new pyranochromene derivative, *Spectrochimica Acta Part A: Mol. and Biomol. Spectroscopy*, 145 (2015) pp. 353-359.

[57] A. Czarny, D. W. Boykin, A. A. Wood, C. M. Nunn, S. Neidle, M. Zhao, W. D. Wilson, Analysis of van der Waals and Electrostatic Contributions in the Interactions of Minor Groove Binding Benzimidazoles with DNA, *J. Am. Chem. Soc*., 117 (1995) pp. 4716–4717.

[58] H. A. Benesi, J. H. Hildebrand, A Spectrophotometric Investigation of the Interaction of Iodine with Aromatic Hydrocarbons, *J. Am. Chem. Soc.*, 71 (1949) pp. 2703-2707.

[59] A. Kathiravan, R. Renganathan, Photoinduced interactions between colloidal TiO2 nanoparticles and calf thymus-DNA, *Polyhedron*, 28 (2009) 1374–1378.

[60] W. Li, J. Xu, X. He, Characterization of the Binding of Methylene Blue to DNA by Spectroscopic Methods, *Anal. Lett*., 33 (2000) pp. 2453–2464.

[61] A. Jaan, W. Iqbal, B. Shahzad, Y. Iqbal, M. U. Rehman, I. Haider, M. T. Javid, U. Anwar, Digest Journal of Nanomaterials and Biostructures, *J. Nanomaterials and Biostruc.*, 17 (2022) pp. 913-920.

[62] A. M. Saleh, Z. A. El–Wahab, O. A. M. Ali, A. A. Faheim, A. A. Salman, Performance of new metal complexes for anionic and cationic dyes photodegradation: construction, spectroscopic studies, optical properties, and DFT calculations, *Res. on Chem. Intermediates*, 49 (2023) pp. 3287–3326.

[63] A.K. Sibhatu, G.K. Weldegebrieal, S. Sagadevan, N.N. Tran, V. Hessel, Photocatalytic activity of CuO nanoparticles for organic and inorganic pollutants removal in wastewater remediation, *Chemosphere*, 300 (2022) pp. 134623.

[64] Z. A. Ujan, A. Tahira, A. A. Mahesar, A. H. Markhand, A. L. Bhatti, A. Q. Mugheri, M. A. Bhatti, N. M. Shaikh, R. H. Mari, A. Nafady, Z. H. Ibupoto, The Crystal Disorder into ZnO with

Addition of Bromine and It's Outperform Role in the Photodegradation of Methylene Blue, *J. Clust. Sci*., 33 (2022) pp. 281-291.